International Journal of Thermal Sciences 48 (2009) 383–390

Contents lists available at ScienceDirect

International Journal of Thermal Sciences

www.elsevier.com/locate/ijts

Analytical solution for non-equilibrium energy transfer in gold: Influence of ballistic contribution of electrons on energy transfer

B.S. Yılbas [a,*], İ.T. Dolapçı [b], M. Pakdemirli [c]

[a] Department of Mechanical Engineering, King Fahd University of Petroleum and Minerals, P.O. Box 1913, Dhahran 31261, Saudi Arabia
[b] Department of Mathematics, Nevşehir University, Nevşehir, Turkey
[c] Department of Mechanical Engineering, Celal Bayar University, 45140 Muradiye, Manisa, Turkey

ARTICLE INFO

Article history:
Received 4 June 2008
Received in revised form 22 September 2008
Accepted 23 September 2008
Available online 15 October 2008

Keywords:
Non-equilibrium
Energy transfer
Gold
Film
Electron
Lattice

ABSTRACT

The analytical solution for non-equilibrium energy transfers in gold substrate and ballistic contribution of electrons to the energy transfer mechanism is examined. The non-equilibrium energy equation including the ballistic contribution of electrons is obtained using the electron kinetic theory approach. The analytical solution using the perturbation method is introduced to formulate lattice and electron temperature distributions in the film. A numerical method using the finite difference scheme is employed to predict and compare electron and lattice site temperatures to those obtained from the analytical solution. It is found that temperature remains high in the surface region of the gold film due to the cases: (i) accounting for the ballistic contribution of electrons to non-equilibrium energy transfer, and (ii) excluding the ballistic contribution to the non-equilibrium energy transfer. This is true for electron and lattice temperatures.

1. Introduction

The short duration of heating across a nano-scaled layer results in a non-equilibrium energy transport in the layer. This causes a thermal separation of electron and lattice subsystems during the short heating period. In this case, electron and lattice site temperatures differ in magnitude and energy transfer is governed in the film through a thermal communication of both subsystems. Moreover, during the short heating period, electron temperature rises due to low specific heat capacity of the electrons and energy transfers from excited electrons to lattice site through the collisional processes. Energy transfer continues in the cooling cycle once the temperature equilibrium is reached between the electron and lattice subsystems. The mathematical model for energy transfer between the electron and lattice subsystems results in high order differential equation. The solution of such equation system is feasible numerical; however, the analytical solution to the problem is fruitful due to reducing the computational efforts. Consequently, investigation into a non-equilibrium energy transfer in the solid substrate and the analytical solution for temperature distribution in the electron and lattice subsystems become necessary.

Considerable research studies were carried out to examine the non-equilibrium energy transfer in solids during the short time periods. The time resolved electron–phonon relaxation in copper was examined by Elsayed-Ali et al. [1]. They indicate that electron–phonon energy transfer was dependent on laser energy and the electron subsystem separates thermally from the lattice subsystem during the heating and cooling periods. The energy transport in thin gold films under the laser heating pulse was examined by Brorson et al. [2]. They indicated that the ballistic electronic motion could contribute to heat transport in the time domain and length scale considered in the analysis. Laser short-pulse heating of metals was investigated by Qiu and Tien [3]. They showed that in the short time-step heating regime, the microscopic energy transfer among photon, electrons, and phonons enlarges the size of the heat affected region and lowers the lattice temperature rise significantly. Laser short-pulse heating and non-equilibrium energy transfer in the solid substrate was examined by Yılbas [4]. He introduced 3-dimensional electron motion in the substrate material and predicted electron and lattice site temperatures numerically. Al-Nimr et al. [6,7] investigated laser short pulse heating process; moreover, the non-equilibrium laser heating of metal films was studied by Al-Nimr and Masood [5]. They used the perturbation technique to uncouple the energy equations. Thermal relaxation of electrons in metals during the short time period was investigated by Allan [8]. He used the standard Bloch–Boltzmann–Peierls formulae to derive an expression for the temperature dependent thermal relaxation rate. The non-equilibrium electron heating in copper was examined by Eesley [9]. He related the transient thermo-modulation spectra of copper with electron temperature.

* Corresponding author.
E-mail address: bsyilbas@kfupm.edu.sa (B.S. Yılbas).

1290-0729/$ – see front matter
doi:10.1016/j.ijthermalsci.2008.09.004

Nomenclature

C_E	electron heat capacity ..... J/m^3 K	β	dimensionless amplitude of volumetric heat source
C_L	lattice heat capacity ..... J/m^3 K	δ	multiplicative inverse of mean free path of electrons 1/m
f	fraction of excess energy change	ε	ratio of heat capacities
G	electron–phonon coupling factor ..... W/m^3 K	ξ	similarity variable
$\bar{I}_0$	dimensional amplitude of exponentially decaying heat source ..... W/m^2	λ	mean free path of electrons ..... m
I_0	dimensionless amplitude of exponentially decaying heat source	μ	dimensionless parameter related to electron mean free time
k	thermal conductivity ..... W/m K	θ_E	dimensionless electron site temperature
k_1	intensity parameter	θ_{E0}	first term in the expansion of dimensionless electron site temperature
m	similarity parameter	θ_{E1}	second term in the expansion of dimensionless electron site temperature
m_0	first term in the perturbation expansion of similarity parameter	θ_L	dimensionless lattice site temperature
m_1	second term in the perturbation expansion of similarity parameter	θ_{L0}	first term in the expansion of dimensionless lattice site temperature
T_E	dimensional electron site temperature ..... K	θ_{L1}	second term in the expansion of dimensionless lattice site temperature
T_L	dimensional lattice site temperature ..... K	θ_0	reference temperature
T_0	reference temperature ..... 300 K	τ_p	electron mean free time between electron–phonon coupling ..... s
t^*	dimensional time ..... s	τ_s	electron–phonon characteristic time ($\tau_s = C_E/G$) ... s
t	dimensionless time		
x^*	dimensional film depth ..... m		
x	dimensionless lattice depth		
α	dimensionless thermal conductivity		

High power laser irradiation of tungsten was investigated by Fujimoto et al. [10]. They suggested that the presence of anomalous heating, a transient non-equilibrium temperature difference between electron and lattice subsystems took place. In addition, an electron–phonon relaxation time of several hundred picoseconds was observed. Chen [11] introduced a ballistic-diffusive equation for the non-equilibrium energy transport in metals. He indicated that the ballistic diffusive equation provided accurate results for the short heating durations. The wave diffusion and parallel non-equilibrium heat conduction in the solids were examined by Honner and Kunes [12]. They introduced the dimensionless criterion of non-equilibrium state to classify the heat transfer situations. Hector et al. [13] investigated the hyperbolic heat conduction due to a mode-locked laser pulsed train. They showed that the hyperbolic model predicted a severe thermal wave front at the surface whereas the parabolic model predicted a continuous temperature rise followed by diffusion of heat into the medium when the pulse train was deactivated. Yılbas [14] investigated laser short-pulse heating including the ballistic contribution of electrons to the non-equilibrium energy transfer process. Moreover, Yılbas et al. [15] and Pakdemirli et al. [16] introduced the analytical solution for the non-equilibrium energy equation using the perturbation method. However the solution was limited to the non-equilibrium energy equation excluding the ballistic contribution of electrons. Consequently, the development of an analytical solution covering ballistic contribution of electrons to the non-equilibrium energy transfer becomes necessary.

In the present study, analytical solution for the non-equilibrium energy transport equation including the ballistic contribution of electrons is carried out using the perturbation method. It should be noted that when the heating duration becomes less or comparable to the thermalization time of the substrate material ($\sim$ picosecond), the ballistic contribution of electrons to the energy transport becomes important [4]; in which case, the use of improved electron kinetic approach becomes essential to accommodate the ballistic contributions. The findings are compared with the results of analytical solution [16] obtained from the same equation excluding the ballistic contribution of electrons. In addition, the predicted numerical solution for the identical boundary and initial conditions are compared with the findings of the present analytical solution. In the model study, a surface heat source applied to a gold substrate is considered and electron as well as lattice site temperature variations in the substrate material are obtained analytically.

2. Mathematical analysis

Recently, Yılbas [14] developed an improved electron kinetic theory formulation for short pulse laser heating

$$\left[\left(1+\tau_s\frac{\partial}{\partial t^*}\right)-\frac{\lambda^2}{f}\frac{\partial^2}{\partial x^{*2}}\right]C_L\frac{\partial T_L}{\partial t^*} = k\frac{\partial^2 T_L}{\partial x^{*2}}+\tau_P\frac{\partial}{\partial t^*}\left(k\frac{\partial^2 T_L}{\partial x^{*2}}\right)+\bar{I}(t)\delta f\exp\left(-\delta|x^*|\right) + \tau_p\frac{\partial}{\partial t^*}\left(\bar{I}(t)\delta f\exp\left(-\delta|x^*|\right)\right) \quad (1)$$

where τ_s is the electron–phonon characteristic time ($\tau_s = C_E/G$), G is the electron–phonon coupling factor, λ is the mean free path of the electrons, f is the fraction of excess energy change, C_L and C_E are the lattice and electron heat capacities, respectively, k is the thermal conductivity, τ_p is the electron mean free time between electron–phonon coupling, $I(t) = \bar{I}_0 g(t)$ where $\bar{I}_0$ is the laser peak power intensity, $g(t)$ is the temporal distribution function of laser pulse, δ is the absorption coefficient. x^* is the lattice depth and t^* is the time variable. T_L and T_E are the lattice site and electron temperatures, respectively.

Introducing the following equalities and dimensionless variables and assuming laser step input pulse intensity ($g(t) = \text{Const.}$)

$$\frac{\lambda^2}{f} = \frac{k\tau_s}{C_E} = \frac{k}{G}, \qquad \tau_s = \frac{C_E}{G}$$
$$\theta_L = \frac{T_L}{T_0}, \qquad \theta_E = \frac{T_E}{T_0}, \qquad x = x^*\delta$$
$$t = \frac{t^*}{C_E/G}, \qquad \varepsilon = \frac{C_E}{C_L}, \qquad \alpha = \frac{k\delta^2}{G} \quad (2)$$

to Eq. (1) yields finally

$$\frac{\alpha(1+\mu)}{\varepsilon}\frac{\partial^3\theta_L}{\partial x^2\partial t}+\alpha\frac{\partial^2\theta_L}{\partial x^2}-\frac{1}{\varepsilon}\frac{\partial^2\theta_L}{\partial t^2}-\frac{1}{\varepsilon}\frac{\partial\theta_L}{\partial t}+\varepsilon\beta\exp(-|x|)+\mu\frac{\partial}{\partial t}\left(\beta\exp(-|x|)\right)=0 \tag{3}$$

where

$$\mu=\frac{\tau_p G}{C_L},\qquad \varepsilon\beta=\frac{\bar{I}_0\delta f}{T_0 G} \tag{4}$$

In the absence of volumetric heat source, $\beta=0$ should be taken and the equation reduces to

$$\frac{\alpha(1+\mu)}{\varepsilon}\frac{\partial^3\theta_L}{\partial x^2\partial t}+\alpha\frac{\partial^2\theta_L}{\partial x^2}-\frac{1}{\varepsilon}\frac{\partial^2\theta_L}{\partial t^2}-\frac{1}{\varepsilon}\frac{\partial\theta_L}{\partial t}=0 \tag{5}$$

This model is the improved energy transport equation including ballistic effects without source in dimensionless form. Once the lattice site temperature is determined, the electron temperature can be found from

$$\theta_E=\theta_L+\frac{1}{\varepsilon}\frac{\partial\theta_L}{\partial t} \tag{6}$$

The previous non-ballistic dimensionless model employed in expressing energy transport for electron and lattice subsystems without source term was [16,17]

$$\frac{\partial\theta_E}{\partial t}=\alpha\frac{\partial^2\theta_E}{\partial x^2}-(\theta_E-\theta_L) \tag{7}$$

$$\frac{\partial\theta_L}{\partial t}=\varepsilon(\theta_E-\theta_L) \tag{8}$$

Elimination of electron temperature between the two equations yield

$$\frac{\alpha}{\varepsilon}\frac{\partial^3\theta_L}{\partial x^2\partial t}+\alpha\frac{\partial^2\theta_L}{\partial x^2}-\frac{1}{\varepsilon}\frac{\partial^2\theta_L}{\partial t^2}-\left(1+\frac{1}{\varepsilon}\right)\frac{\partial\theta_L}{\partial t}=0 \tag{9}$$

An analytical solution of Eqs. (7) and (8), which is also a solution of (9), using Lie Group theory combined with perturbations was presented before [16]. The goal will be to compare the solutions of improved (Eq. (5)) and previous (Eq. (9)) models. In a variety of applications, dimensionless thermal conductivity α is of order 1 and the ratio of heat capacities ε is small compared to order 1 terms. It should be noted that if ε is of order 1 or greater, then application of the perturbation method fails to predict the correct temperature distribution. Therefore, as will be shown later, a perturbation type of solution in terms of the small parameter ε is possible. Before applying perturbations, in the next section, the symmetries of the model will be calculated first. This will enable us to transfer the model from a partial differential system to an ordinary differential system. A perturbation solution of the ordinary differential system will follow then.

3. Symmetries and a similarity transformation

Lie Group theory [18–20] will be applied to Eq. (5). The infinitesimal generator for the problem can be written as

$$X=\xi_1\frac{\partial}{\partial x}+\xi_2\frac{\partial}{\partial t}+\eta\frac{\partial}{\partial\theta_L} \tag{10}$$

In the standard procedure, Eq. (9) is re-written using higher order variables as follows

$$\frac{\alpha(1+\mu)}{\varepsilon}u_{112}+\alpha u_{11}-\frac{1}{\varepsilon}u_{22}-\frac{1}{\varepsilon}u_2=0 \tag{11}$$

where new variables are defined for convenience

$$x_1=x,\qquad x_2=t,\qquad u=\theta_L$$
$$u_2=\frac{\partial\theta_L}{\partial x_2},\qquad u_{11}=\frac{\partial^2\theta_L}{\partial x_1^2}$$
$$u_{22}=\frac{\partial^2\theta_L}{\partial x_2^2},\qquad u_{112}=\frac{\partial^3\theta_L}{\partial x_1^2\partial x_2} \tag{12}$$

Generator (10) is prolonged to higher order variables

$$X=\xi_1\frac{\partial}{\partial x_1}+\xi_2\frac{\partial}{\partial x_2}+\eta\frac{\partial}{\partial u}+\eta_2^{(1)}\frac{\partial}{\partial u_2}+\eta_{11}^{(2)}\frac{\partial}{\partial u_{11}}+\eta_{22}^{(2)}\frac{\partial}{\partial u_{22}}+\eta_{112}^{(3)}\frac{\partial}{\partial u_{112}} \tag{13}$$

Applying the prolonged generator to Eq. (11) yields the invariance condition

$$\frac{\alpha(1+\mu)}{\varepsilon}\eta_{112}^{(3)}+\alpha\eta_{11}^{(2)}-\frac{1}{\varepsilon}\eta_{22}^{(2)}-\frac{1}{\varepsilon}\eta_2^{(1)}=0 \tag{14}$$

$\eta_2^{(1)},\eta_{22}^{(2)},\eta_{11}^{(2)},\eta_{112}^{(3)}$ are to be expressed in terms of ξ_1,ξ_2,η using the standard recursion formulas [18–20]. The invariance conditions can be treated as polynomials in terms of defined higher order variables. Hence, equating the coefficients of those polynomials on both sides yields a set of over-determined partial differential system. Solving the over-determined partial differential system and returning back to the original variables yield

$$\xi_1=a$$
$$\xi_2=b \tag{15}$$
$$\eta=c\theta_L+D(x,t)$$

where the structure of $D(x,t)$ is determined by the below equation

$$\frac{\alpha(1+\mu)}{\varepsilon}\frac{\partial^3 D}{\partial x^2\partial t}+\alpha\frac{\partial^2 D}{\partial x^2}-\frac{1}{\varepsilon}\frac{\partial^2 D}{\partial t^2}-\frac{1}{\varepsilon}\frac{\partial D}{\partial t}=0 \tag{16}$$

Parameters a, b and c represent finite Lie point symmetries whereas $D(x,t)$ is an infinite Lie point symmetry.

Similar calculations for the previous model of Eq. (9) produces exactly the same symmetries given in (15) with the structure of $D(x,t)$ determined by the equation

$$\frac{\alpha}{\varepsilon}\frac{\partial^3 D}{\partial x^2\partial t}+\alpha\frac{\partial^2 D}{\partial x^2}-\frac{1}{\varepsilon}\frac{\partial^2 D}{\partial t^2}-\left(1+\frac{1}{\varepsilon}\right)\frac{\partial D}{\partial t}=0 \tag{17}$$

From the symmetries, a similarity solution can be constructed using the parameters a and b and selecting $c=0$, $D(x,t)=0$. The determining equations for this choice is

$$\frac{dx}{a}=\frac{dt}{b}=\frac{d\theta_L}{0} \tag{18}$$

Solving the system, the similarity variable and functions are determined

$$\xi=x-mt,\qquad \theta_L=\theta_L(\xi) \tag{19}$$

where $m=a/b$. Substituting the variables into Eq. (5) yields

$$\alpha(1+\mu)\theta_L'''+\left(m-\varepsilon\frac{\alpha}{m}\right)\theta_L''-\theta_L'=0 \tag{20}$$

where prime denotes differentiation with respect to the similarity variable ξ. Using Eq. (6), the electron temperature in terms of similarity variables is

$$\theta_E=-\frac{m}{\varepsilon}\theta_L'+\theta_L \tag{21}$$

Following a similar procedure for Eq. (9), one has

$$\alpha\theta_L'''+\left(m-\varepsilon\frac{\alpha}{m}\right)\theta_L''-(1+\varepsilon)\theta_L'=0 \tag{22}$$

4. Perturbation solution

In a variety of applications, the ratio of heat capacities (i.e. parameter ε) is rather small (in the order of 10^{-2}), hence a perturbation type of solution is possible. Since the straightforward expansion breaks down due to secular terms, strained parameters method will be employed [21]. In accordance, the dependent variable as well as the similarity parameter m is expanded in a perturbation series

$$\theta_L = \theta_{L0} + \varepsilon\theta_{L1} + \cdots \tag{23}$$

$$m = m_0 + \varepsilon m_1 + \cdots \tag{24}$$

Inserting the expansions into Eq. (20) and separating at each order yields

$$O(1): \quad \alpha(1+\mu)\theta_{L0}''' + m_0\theta_{L0}'' - \theta_{L0}' = 0 \tag{25}$$

$$O(\varepsilon): \quad \alpha(1+\mu)\theta_{L1}''' + m_0\theta_{L1}'' - \theta_{L1}' = -m_1\theta_{L0}'' + \frac{\alpha}{m_0}\theta_{L0}'' \tag{26}$$

The solution at order 1 is

$$\theta_{L0} = c_1 + c_2 e^{\lambda_1\xi} + c_3 e^{\lambda_2\xi} \tag{27}$$

where

$$\lambda_1 = \frac{-m_0 - \sqrt{m_0^2 + 4\alpha(1+\mu)}}{2\alpha(1+\mu)}$$

$$\lambda_2 = \frac{-m_0 + \sqrt{m_0^2 + 4\alpha(1+\mu)}}{2\alpha(1+\mu)} \tag{28}$$

For decaying type of solutions, $c_3 = 0$ should be selected. Inserting this solution into the next order and eliminating secular terms yields

$$m_1 = \frac{\alpha}{m_0} \tag{29}$$

Returning back to the original variables, calculating θ_E from Eq. (21), the approximate solutions can be written as follows

$$\theta_L = c_1 + c_2 e^{\lambda_1(x-mt)} + \cdots \tag{30}$$

$$\theta_E = c_1 + c_2\left(1 - \frac{m}{\varepsilon}\lambda_1\right)e^{\lambda_1(x-mt)} + \cdots \tag{31}$$

$$m = m_0 + \varepsilon\frac{\alpha}{m_0} + \cdots$$

$$\lambda_1 = \frac{-m_0 - \sqrt{m_0^2 + 4\alpha(1+\mu)}}{2\alpha(1+\mu)} \quad \text{(improved formulation)} \tag{32}$$

For the previous model represented by Eq. (9) and further by (22), solutions (30) and (31) are still valid with only m and λ_1 parameters being different

$$m = m_0 + \varepsilon\left(\frac{\alpha}{m_0} - \frac{2\alpha}{m_0 + \sqrt{m_0^2 + 4\alpha}}\right) + \cdots$$

$$\lambda_1 = \frac{-m_0 - \sqrt{m_0^2 + 4\alpha}}{2\alpha}$$

(previous formulation [14]) (33)

The analytical solutions are valid for $\varepsilon \ll 1$.

5. A boundary value problem and time condition

A surface heat source is applied at $t = 0$. Totally 4 conditions are needed to solve the equations. Since the equations are coupled, some of them are for lattice and some of them are for electron temperatures. Instead of time conditions at the beginning, time conditions at infinity are given from the physics of the problem. Electron and lattice temperatures are assumed to be the same as the reference temperature ($\theta_E = \theta_0$ and $\theta_L = \theta_0$, where θ_0 is a reference temperature) at time approaches to infinity ($t = \infty$). Moreover, a semi infinite substrate material heated with a time decaying source from the surface is assumed. The boundary and time conditions for the problem can be written as follows

$$\frac{\partial\theta_E(0,t)}{\partial x} = -I_0 e^{-k_1 t}, \qquad \frac{\partial\theta_E(\infty,t)}{\partial x} = 0$$

$$\theta_E(x,\infty) = \theta_0, \qquad \theta_L(x,\infty) = \theta_0 \tag{34}$$

The dimensionless source amplitude I_0 is related to the dimensional one $\bar{I}_0$ through the relation $I_0 = \bar{I}_0/(k\delta T_0)$. For the above boundary conditions, the approximate solutions are finally found to be

$$\theta_E = \theta_0 - \frac{I_0}{\lambda_1}e^{\lambda_1[x-(m_0+\varepsilon m_1)t]} \tag{35}$$

$$\theta_L = \theta_0 - \frac{I_0}{\lambda_1\left[1 - \left(m_1 + \frac{m_0}{\varepsilon}\right)\lambda_1\right]}e^{\lambda_1[x-(m_0+\varepsilon m_1)t]} \tag{36}$$

The dependence of the similarity parameter m on the decay rate is given by the relation

$$\lambda_1 m = k_1 \tag{37}$$

These final solutions are valid for both formulations provided that Eq. (32) is used for parameter definitions in the improved formulation and Eq. (33) for the previous formulation.

6. Validation of improved electron kinetic theory model

To validate the improved electron kinetic theory model, the transient reflectivity data given in the previous study [22] are considered. It should be noted that in the early heating period, the lattice temperature change is considerably small and the surface reflectivity change is due to electron temperature rise in this period. In this case, the reflectivity change can be related with the electron temperature change [20], i.e.:

$$\frac{\Delta R}{(\Delta R)_{\max}} = \frac{\Delta T_E}{(\Delta T_E)_{\max}} \tag{38}$$

In order to proceed with the comparison, the experimental condition including the laser pulse used in the experiment is employed in the simulations [22]. Since the laser source is volumetric, Eq. (1) is employed in the simulations. In the previous experiment, the laser source was a colliding-pulse mode-locked (CPM) dye laser with a wavelength 630 nm [20]. The laser source term is [22]:

$$I(t) = 0.94\frac{1-r_f}{t_p}\delta J \exp\left(-x\delta - 2.77\left(\frac{t}{t_p}\right)^2\right) \tag{39}$$

where t_p is full width-at-half-maximum (FWHM) duration of the laser pulse, and $t = 0$ is defined at the moment when the peak of a laser pulse arrives at the metal surface. J is the total energy carried by a laser pulse divided by the cross-sectional area of the laser spot. In the validation simulations, $t_p = 96$ femtoseconds and $J = 10$ J/m^2 are used [22].

Fig. 1 shows the temporal variation of the normalized reflectivity change obtained from the experiment and predicted from two equation as well as improved electron kinetic theory approach

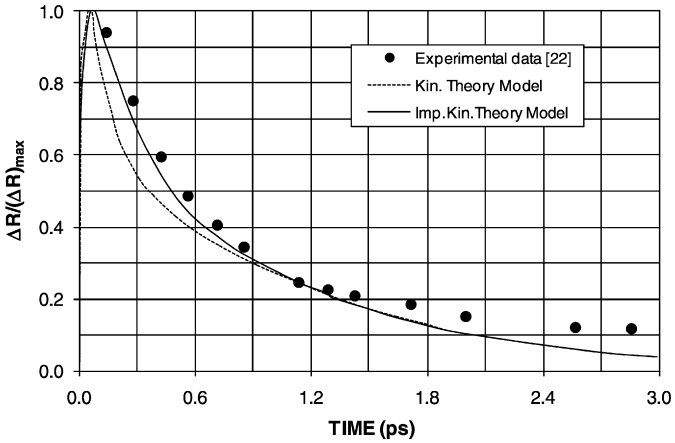

Fig. 1. Temporal variation of normalized reflectivity change obtained from the improved electron kinetic theory model and the previous study [22].

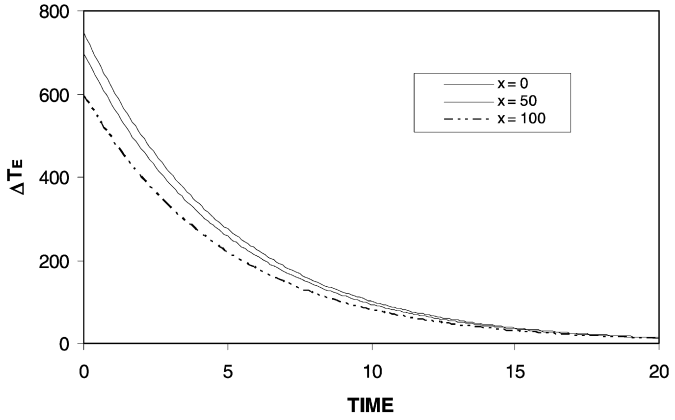

Fig. 2. Temporal variation of dimensionless electron temperature difference at three non-dimensional depths in the substrate material. Temperature difference is due to the cases for ballistic and non-ballistic contribution of electrons to the energy transfer.

Table 1
Thermo-physical properties of gold at 300 K and numerical values of parameters used.

Property	Numerical value
C_L	2.8×10^6 J/m^3 K
C_E	2.1×10^4 J/m^3 K
G	2.6×10^{16} W/m^3 K
k	315 W/m K
δ	1×10^9 m^{-1}
τ_p	0.024×10^{-12} s
T_0	300 K

Table 2
Dimensionless parameter values used in the analysis.

Parameter	Numerical value
ε	7.5×10^{-3}
α	12115.4
μ	2.229×10^{-4}
k_1	0.2
I_0	3.175

for gold film. It is evident that the improved electron kinetic theory approach and two equation model predict similar normalized reflectivity. Moreover, the results obtained from the improved electron kinetic theory approach give slightly closer results to experimental data as compared to that corresponding to the two-equation model, particularly for time period less than 1 ps.

7. Results and discussion

A non-equilibrium energy transport in a gold substrate heated by a heat source at the free surface is considered. In the analysis, ballistic contribution of electrons to the energy transfer is considered when formulating the non-equilibrium energy exchange between the electron and the lattice subsystems. A perturbation method is used to obtain the analytical solution for electron and lattice site temperatures. A comparison between temperature predictions in the lattice and electron subsystem due to ballistic and non-ballistic cases is made. The dimensional and dimensionless parameter values used in the analysis are given in Tables 1 and 2, respectively. Moreover dimensionless time $t = 5$ corresponds to 4.04×10^{-12} s and dimensionless distance 500 corresponds to 5×10^{-7} m below the surface.

Fig. 2 shows temporal variation of dimensionless electron temperature difference resulted from ballistic and non-ballistic contribution in the energy transfer equation. Dimensionless temperature difference is high in the early heating period and it decreases with progressing time. The rate of decay of temperature difference in the early heating period ($t \leqslant 4$) is rapid and as the time progresses further difference due to the ballistic and non-ballistic contributions is associated with the electron excess energy gained from the heat source and electron excess energy transfer to the lattice site. In this case, the fast moving electrons in the surface region gains extra energy from the heat source and loss small fraction of their excess energy to the lattice site through the collisional process, provided that in a short duration the amount of excess energy transfer to the lattice subsystem becomes less due to a few number of collisions. This results in attainment of high electron temperature due to the ballistic contribution of the electrons. However, as the time progresses, electron excess energy gain increases, particularly at the surface because of the high rate of energy transfer from the surface, i.e., heat source is located at the surface. This results in reduction in temperature difference due to the ballistic and the non-ballistic contributions of electrons. In addition, the number of collisions taking place between the electron and lattice subsystems increase with the progressing time. This contributes to the reduction in electron temperature difference. However, as the depth below the surface increases, difference in electron temperature becomes less in magnitude, provided that the behavior of decay rate of temperature difference does not change much from that at the surface. The reduction in electron temperature difference at some depth below the surface is attributed to the amount of electron excess energy gain from the surface; in which case, electron gains energy at the surface due to the location of heat source.

Fig. 3 shows temporal variation of dimensionless lattice site temperature difference at three locations in the substrate material. Moreover, lattice temperature attains lower values for the case of the ballistic contribution than that for the non-ballistic contribution. It should be noted that temperature difference corresponds to lattice site temperature obtained from the non-ballistic contribution minus that of ballistic contribution. Temperature difference is high in the early heating period and reduces with progressing time, which is more pronounced in the surface region. The attainment of large difference in lattice site temperature is due to the attainment of high electron temperature for the case of ballistic contribution. It should be noted that lattice site temperature is low in the early heating period due to small number of collisions taking place between the lattice site and electrons. Although lattice site temperature is low during the early heating period, temperature difference becomes high. In this case, electron phonon coupling is suppressed by the ballistic motion of electrons while reducing the amount of electron excess energy transfer to

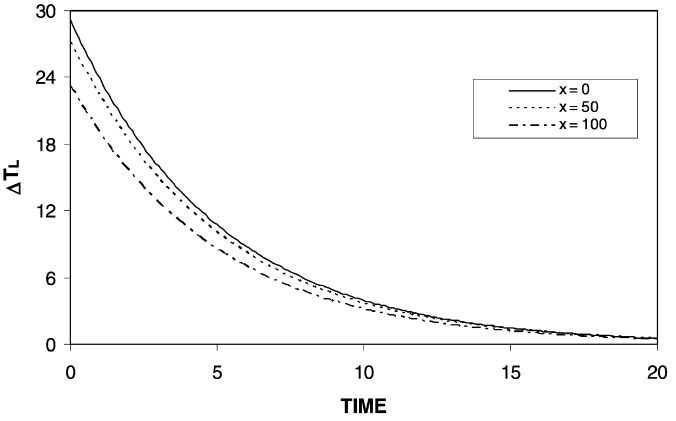

Fig. 3. Temporal variation of dimensionless lattice temperature difference at three non-dimensional depths in the substrate material. Temperature difference is due to the cases for ballistic and non-ballistic contribution of electrons to the energy transfer.

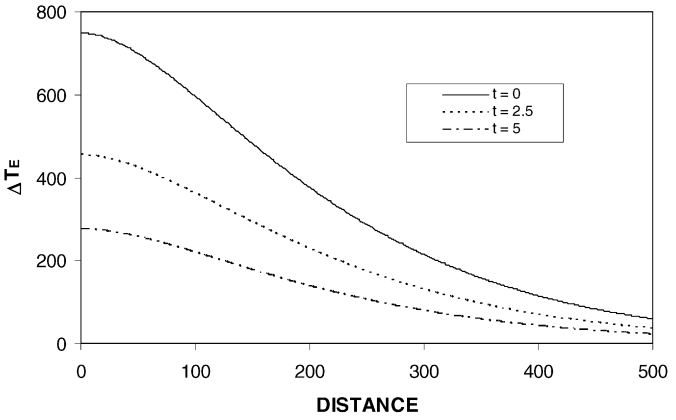

Fig. 4. Non-dimensional electron temperature difference inside the substrate material at three periods. Temperature difference is due to the cases for ballistic and non-ballistic contribution of electrons to the energy transfer.

the lattice site through the collisional process. Consequently, lattice site temperature becomes low while electron temperature remains high in the early heating period, particularly for the case of the ballistic contribution. As the heating period progresses, electron excess energy gained from the surface and the number of collisions between electrons and lattice site increases. This situation alters the electron phonon coupling mechanism and electron excess energy transfer to the lattice site enhances, which in turn reduces the temperature difference, due to ballistic and non-ballistic contribution cases, in the lattice site. Moreover, the decay rate of lattice site temperature difference follows almost the decay rate of electron temperature difference, noted that the magnitude of the decay rate changes due to the differences in the specific heat capacities of electrons and the lattice site. Consequently, the ballistic contribution of electrons on the energy transport becomes significant in the early heating periods at which the duration is short. However, progressing time minimizes this effect on the non-equilibrium energy transfer. As the depth below the surface increases, difference in lattice site temperature reduces due to a small fraction of electron excess energy transfer to the lattice site through the collisional process with increasing depth. In this case, electron excess energy gain from the surface source reduces with increasing depth below the surface.

Figs. 4 and 5 show dimensionless electron and lattice temperature differences in the substrate material for three time periods. Temperature difference is high in the surface region and decays with increasing depth below the surface, which is true for all the

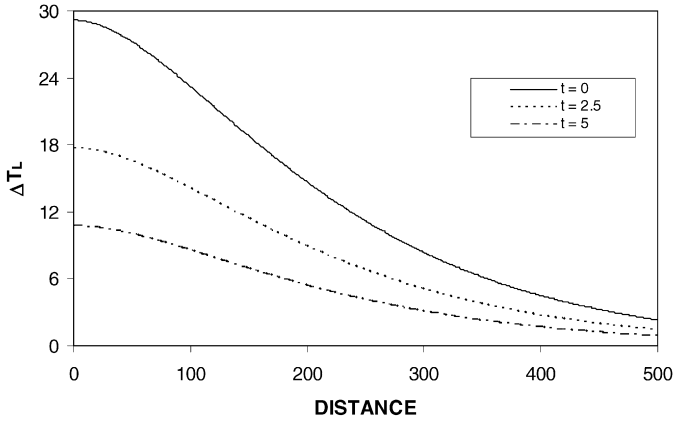

Fig. 5. Non-dimensional lattice temperature difference inside the substrate material at three periods. Temperature difference is due to the cases for ballistic and non-ballistic contribution of electrons to the energy transfer.

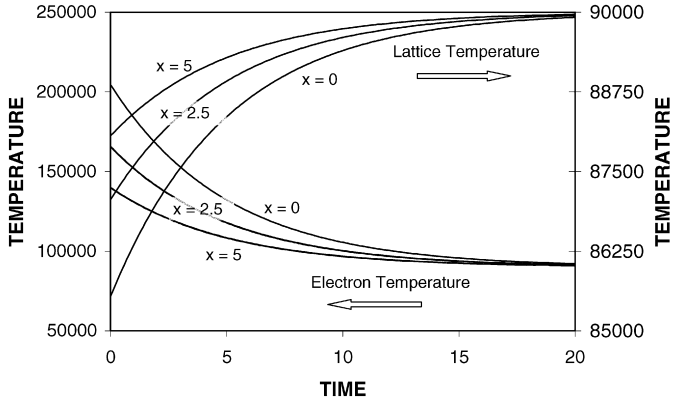

Fig. 6. Temporal variation of dimensionless electron and lattice temperatures at three non-dimensional depths in the substrate material.

heating periods considering in the simulations. The attainment of temperature difference in the surface region is associated with electron excess energy gain from the surface. However, once the electron excess energy decreases with increasing depth so that the temperature difference, which becomes less for both the cases of ballistic and non-ballistic contributions. As the heating period progresses, electron phonon coupling alters due to high electron excess energy gain and the increased number of collisions between electrons and the lattice site. This in turn, modifies the gradient of temperature difference along the depth. In this case, the gradient of temperature difference becomes smaller for long heating periods as compared to that corresponding to the early heating period. In the case of temperature difference for the lattice site (Fig. 5) temperature difference decays with increasing depth below the surface. Although lattice temperature difference decay follows the trend of electron temperature difference, the gradients of both distributions are different. Moreover, the attainment of low gradient for the lattice site temperature difference for during the long heating period is associated with the high number of electron and the lattice site collisions as well as improved electron–phonon coupling at high electron temperatures (Eq. (33)).

Fig. 6 shows temporal variation of non-dimensional electron and lattice site temperature distributions, which were obtained from Eqs. (31) and (30) at three depths. Lattice site temperature increases while electron temperature decreases with progressing time. This is because of the energy exchange mechanism taking place between electrons and lattice site. Moreover, this process continues until the electron and the lattice subsystems reach the temperature equilibrium. The rise of lattice site temperature and

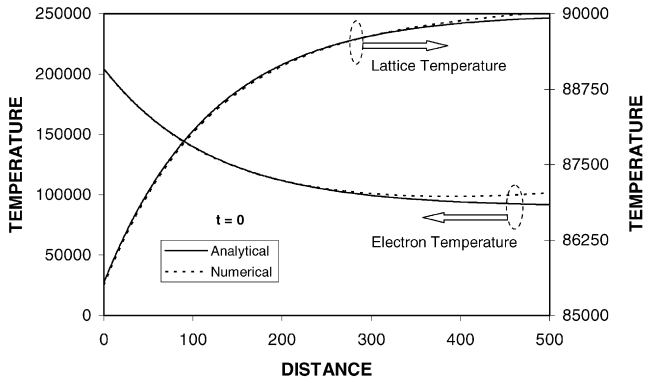

Fig. 7. Dimensionless electron and lattice temperatures in the substrate material for three heating periods.

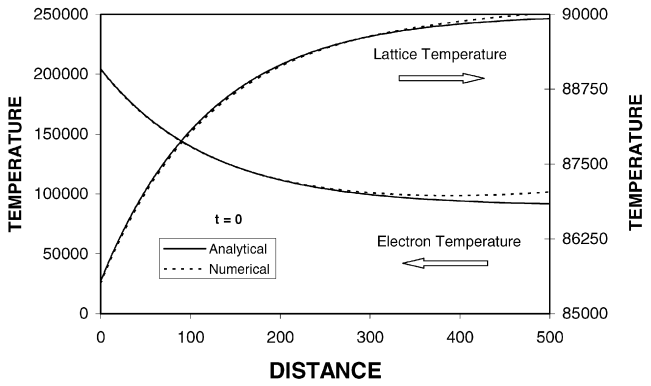

Fig. 8. Comparison of dimensionless electron and lattice site temperatures obtained from the analytical solution and predicted numerically.

decay rate of electron temperature is high in the early heating period. This situation is more pronounced in the surface region. The attainment of high temperature rise in lattice temperature and high decay rate in electron temperature are associated with the energy transfer to electrons at the surface and energy exchange mechanism through the collisional process. In this case, energy gain by electrons at the surface results in rapid rise of electron excess energy in the surface region and as the time progresses electron excess energy transfers to the lattice site while reducing electron excess energy. This results in rapid decay of electron excess energy, particularly in the surface region. Moreover, the heat source at the surface decays with time, electron temperature reduces significantly at the surface with progressing time. Consequently, energy transfer through the collisional process from the excited electrons and energy gain by electrons from the surface heat source at the free surface, which decays with time, are responsible for the rapid decay of electron temperature in the surface region. In the early heating period, lattice site temperature is low and energy transfer from electrons to lattice site through the collisional process enhances lattice site temperature with progressing time. As the distance increases from the surface, the rate of temperature decay in electron temperature and rate of rise in lattice site temperature reduce due to low electron excess energy in these regions. It should be noted that electron loss energy starting from the surface region towards the solid bulk through the collisional process.

Fig. 7 shows non-dimensional electron and lattice site temperatures in the substrate material for three time periods. Electron temperature decays sharply while lattice temperature increases in the surface region of the substrate material. This is because of the heat source located at the free surface of the substrate material; therefore, energy gain by electrons at the surface is high. This gives rise to attainment of high electron temperature at the surface. Moreover, electrons transfer their excess energy to lattice site through the collisional process. This enhances temperature rise in the lattice subsystem. Since electrons transfer some portion of their excess energy to the lattice site in the surface region and heat source is located at the free surface, electron excess energy reduces with increasing depth below the surface. Moreover, electrons transfer their excess energy up to the point when the both subsystems reach temperature equilibrium. Consequently, as electrons depart from the surface region towards the solid bulk, they continuously transfer their excess energy to the lattice site unless the lattice site and electron are in temperature equilibrium. Moreover, the amount of electron excess energy transfer to lattice becomes low as the depth below the surface increases. This lowers the rise of lattice site temperature at some depth below the surface, i.e. temperature rise becomes gradual.

To compare the results of analytical solutions (Eqs. (30) and (31)), a numerical method using the finite difference scheme is introduce to discretize the governing equations of energy (Eq. (5)). In the numerical simulations, identical boundary and initial conditions, which were used in the analytical solutions, are adopted. In addition, the same material properties, which were used for the analytical solutions, are employed in the simulations.

Fig. 8 shows comparison of non-dimensional electron and lattice temperatures obtained from Eqs. (30), (31) and predicted numerically. It can be observed that both results are in a very good agreement. However, some small difference at some depth below the surface is due to the numerical convergence, which is associated with the numerical residuals. This gives rise to small residuals, which contribute to the numerical errors in this region. Nevertheless, the agreement is excellent in particular at high temperatures, which occur in the surface region.

8. Conclusions

Non-equilibrium energy transfer in gold substrate is considered and the analytical solution using the perturbation method is introduced to obtain electron and lattice site temperature distributions. The influence of ballistic contribution of electrons on the non-equilibrium energy transport is examined through computing the temperature difference between two cases; (i) accounting the ballistic contribution and (ii) excluding the ballistic contribution. The governing non-equilibrium energy equation is solved numerically to compare the results of the analytical solution. It is found that electron temperature decay is sharp while lattice site temperature is high in the surface region of the substrate material. This is because of the electron excess energy transfer to the lattice site through the collisional process and the heat source located at the surface. However, as the depth increases away from the surface, electron temperature decay and lattice site temperature increase become gradual. In this case, electron leaving surface towards the solid bulk transfers some of their excess energy before reaching the solid bulk of the substrate material. Consequently, less electron excess energy results in less rise of lattice site temperature through the collisional process in this region. Electron temperature difference, due to the cases of ballistic contribution and no ballistic contribution, becomes high in the surface region where electron excess energy remains high in this region. However, as the distance increases towards the bulk of the substrate material, electron temperature difference becomes less. This reveals that ballistic contribution of electrons to the non-equilibrium energy transport becomes significant when electron excess energy becomes high. Moreover, lattice site temperature difference, due to the cases of ballistic and non-ballistic contributions, becomes high in the surface region of the gold where electron excess energy is

also high. Consequently, ballistic contribution of electrons to the non-equilibrium energy transport results in attainment of high lattice site temperature. When comparing the numerical predictions of electron temperature to that determined from the analytical solution, it is evident that both results are in a good agreement.

Acknowledgements

The authors acknowledge the support of TÜBİTAK under project no: 104T514. B.S. Yılbas acknowledges the support of King Fahd University of Petroleum and Minerals.

References

[1] H.E. Elsayed-Ali, T.B. Norris, M.A. Pessot, G.A. Mourou, Time-resolved observation of electron–phonon relaxation in copper, Physical Review Letters 58 (1987) 1212–1215.
[2] S.D. Brorson, A. Kazeroonian, J.S. Moodera, D.W. Face, T.K. Cheng, E.P. Ippen, M.S. Dresselhaus, G. Dresselhaus, Femtosecond room-temperature measurement of the electron–phonon coupling constant λ in metallic superconductors, Physical Review Letters 64 (1990) 2172–2175.
[3] T.Q. Qiu, C.L. Tien, Femtosecond laser heating of multi-layer metals—I. Analysis, Int. J. Heat Mass Transfer 37 (17) (1994) 2789–2797.
[4] B.S. Yılbas, Electron kinetic theory approach—one- and three-dimensional heating with pulsed laser, Int. J. Heat Mass Transfer 44 (2001) 1925–1936.
[5] M.A. Al-Nimr, S.A. Masoud, Nonequilibrium laser heating of metal films, ASME, J. Heat Transfer 119 (1997) 188–190.
[6] M.A. Al-Nimr, M. Alkam, V. Arpaci, Heat transfer mechanisms during short-pulse laser heating of two-layer composite thin films, Heat and Mass Transfer 38 (7–8) (2002) 609–614.
[7] M.A. Al-Nimr, B.A. Abu-Hijleh, M.A. Hader, Effect of thermal losses on the microscopic hyperbolic heat conduction model, Heat and Mass Transfer 39 (3) (2003) 201–207.
[8] P.B. Allen, Theory of thermal relaxation of electrons in metals, Physical Review Letters 59 (1987) 1460–1463.
[9] G.L. Eesley, Generation of nonequilibrium electron and lattice temperatures in copper by picosecond laser pulses, American Physical Society 33 (1986) 2144–2151.
[10] J.G. Fujimoto, J.M. Liu, E.P. Ippen, Femtosecond laser interaction with metallic tungsten and nonequilibrium electron and lattice temperatures, Physical Review Letters 53 (1984) 1837–1840.
[11] G. Chen, Ballistic-diffusive heat-conduction equations, Physical Review Letters 86 (2001) 2297–2300.
[12] M. Honner, J. Kunes, On the wave diffusion and parallel nonequilibrium heat conduction, ASME, J. Heat Transfer 121 (1999) 702–707.
[13] L.G. Hector Jr., W.S. Kim, M.N. Ozisik, Hyperbolic heat conduction due to mode locked laser pulse train, Int. J. Engng. Sci. 30 (1992) 1731–1744.
[14] B.S. Yılbas, Improved formulation of electron kinetic theory approach for laser short-pulse heating, Int. J. Heat Mass Transfer 49 (13–14) (2006) 2227–2238.
[15] B.S. Yılbas, M. Pakdemirli, Analytical solution for temperature field in electron and lattice sub-systems during heating of solid film, Physica B: Condensed Matter 382 (1–2) (2006) 213–219.
[16] M. Pakdemirli, İ.T. Dolapçı, B.S. Yılbas, Symmetries and approximate solution of energy transfer equations in short pulse laser heating, International Journal of Thermal Sciences 46 (2007) 908–913.
[17] B.S. Yılbas, M. Pakdemirli, S. Bin Mansoor, Analytical solution for temperature field in thin film initially heated by a short-pulse laser source, Heat and Mass Transfer 41 (2005) 1077–1084.
[18] G.W. Bluman, S. Kumei, Symmetries and Differential Equations, Springer-Verlag, New York, 1989.
[19] N.H. Ibragimov, CRC Handbook of Lie Group Analysis of Differential Equations, vols. 1–3, CRC Press, Boca Raton, FL, 1994.
[20] H. Stephani, Differential Equations: Their Solutions Using Symmetries, Cambridge University Press, Cambridge, 1989.
[21] A.H. Nayfeh, Introduction to Perturbation Techniques, John Wiley and Sons, New York, 1981.
[22] D.Y. Tzou, K.S. Chiu, Temperature-dependent thermal lagging in ultrafast laser heating, Int. J. Heat Mass Transfer 44 (2001) 1725–1734.